



Application of Positron Annihilation Lifetime Spectroscopy (PALS) to Study the Nanostructure in Amphiphile Self-Assembly Materials: Phytantriol Cubosomes and Hexosomes

Journal:	<i>Physical Chemistry Chemical Physics</i>
Manuscript ID:	CP-ART-09-2014-004343.R1
Article Type:	Paper
Date Submitted by the Author:	05-Nov-2014
Complete List of Authors:	Fong, Celesta; CSIRO, Manufacturing Flagship Drummond, Calum; RMIT University, School of Applied Sciences Hill, Anita; CSIRO, Manufacturing Flagship Waddington, Lynne; CSIRO, Manufacturing Flagship Dong, Aurelia; CSL, Boyd, Ben; Monash University, Monash Institute of Pharmaceutical Sciences

Application of Positron Annihilation Lifetime Spectroscopy (PALS) to Study the Nanostructure in Amphiphile Self-Assembly Materials: Phytantriol Cubosomes and Hexosomes

Aurelia W. Dong,^{1,2} Celesta Fong,² Lynne J. Waddington,³ Anita J. Hill,² Ben J Boyd^{1,4*} and Calum J. Drummond^{2,5*}.

¹ Drug Delivery, Disposition and Dynamics, Monash Institute of Pharmaceutical Sciences, Monash University (Parkville Campus), 381 Royal Parade, Parkville, VIC 3052, Australia

² CSIRO Manufacturing Flagship, Private Bag 10, Clayton, VIC 3169, Australia

³ CSIRO Manufacturing Flagship, 343 Royal Parade, Parkville, VIC 3052, Australia

⁴ ARC Centre of Excellence in Convergent Bio-Nano Science and Technology, Monash Institute of Pharmaceutical Sciences, Monash University (Parkville Campus), 381 Royal Parade, Parkville, VIC 3052, Australia

⁵ School of Applied Sciences, College of Science Engineering and Health, GPO Box 2476, RMIT University, Melbourne, VIC 3001, Australia

Corresponding Authors: calum.drummond@rmit.edu.au; ben.boyd@monash.edu

Abstract

Self-assembled amphiphile nanostructures of colloidal dimensions such as cubosomes and hexosomes are of interest as delivery vectors in pharmaceutical and nanomedicine applications. Translation would be assisted through a better understanding of the effects of drug loading on the internal nanostructure, and the relationship between this nanostructure and drug release profile. Positron Annihilation Lifetime Spectroscopy (PALS) is sensitive to local microviscosity and is used as an *in-situ* molecular probe to examine the Q₂ (cubosome) → H₂ (hexosome) → L₂ phase transitions of the pharmaceutically relevant phytantriol/ water system in the presence of a model hydrophobic drug, vitamin E acetate (VitEA). It is shown that the orthopositronium lifetime (τ) is sensitive to molecular packing and mobility and this has been correlated with the rheological properties of individual lyotropic liquid crystalline mesophases. Characteristic PALS lifetimes for L₂ ($\tau_4 \sim 4$ ns) \sim H₂ ($\tau_4 \sim 4$ ns) $>$ Q₂ Pn3m ($\tau_4 \sim 2.2$ ns) are observed for the phytantriol/water system, with the addition of VitEA yielding a gradual increase in τ from $\tau \sim 2.2$ ns for cubosomes to $\tau \sim 3.5$ ns for hexosomes. The dynamic chain packing at higher temperatures and in the L₂ and H₂ phases is qualitatively less “viscous,” consistent with rheological measurements. This information offers increased understanding of the relationship between internal nanostructure and species permeability.

Keywords: Positron annihilation lifetime spectroscopy, phytantriol, cubosome, hexosome, hydrophobic drug, vitamin E acetate

Introduction

There has been a burgeoning of potential drug candidates in recent years resulting from advances in automated synthesis and combinatorial chemistry. However successful drug development relies on efficient delivery to targeted sites and this requires a thorough understanding of the structure and characteristics of cellular barriers and the mechanisms of drug diffusion and permeability through encapsulation materials.

The spontaneous self-assembly of amphiphilic molecules in water to create thermodynamically stable complex nanostructures has been used for this purpose, [1-3] [4] with colloidal dispersions of self-assembled liquid crystals with two- and three- dimensional order such as cubosomes and hexosomes used for solubilisation[5, 6] and as delivery vectors in pharmaceutical[4, 7-9] [10-13] and food applications.[14-18] The internal nanostructure of these lyotropic liquid crystalline dispersions of particles closely resembles that of the non-dispersed lyotropic liquid crystal mesophases from which they are derived, namely the inverse bicontinuous cubic phase (Q_2) and inverse hexagonal phase (H_2). These colloidal dispersions are analogous to liposomes and afford a flowable precursor with high surface area for *in vivo* application.

The utility of such matrices as encapsulants lies in their inherent nanostructure with differences between Q_2 and H_2 morphology used to underpin strategies for controlling the molecular mobility and availability of the drug. The morphology of the self-assembled structures is therefore important for their final application. [19, 20] [11, 21, 22] The tortuosity and high surface area ($400 \text{ m}^2/\text{g}$)[4] of the Q_2 phase arises from a continuous amphiphile bilayer draped over a surface which subdivides space into two non-interpenetrating, congruent water networks; whereas the H_2 phase comprises a hexagonally close packed arrangement of infinitely long rod-like micelles.[1] High tortuosity and surface area are two criteria often cited as important in the use of the Q_2 phase for controlled release applications, [4, 20] whereas the end-capped cylindrical aqueous micelles of the H_2 provide a significantly hindered path for diffusion, resulting in slower release kinetics.

Given the interest in these matrices as drug delivery vectors, there is an increasing desire for a detailed molecular understanding of how the void spaces and nanostructure may assist in elucidating the specific relationship between permeability and diffusion-dependent transport

from these matrices. Of particular interest is how the total amount and size distribution of the void volume is governed by the molecular composition of the host matrix; and further how these impact diffusion of the encapsulate as a function of phase transitions arising from changes to the external environment.

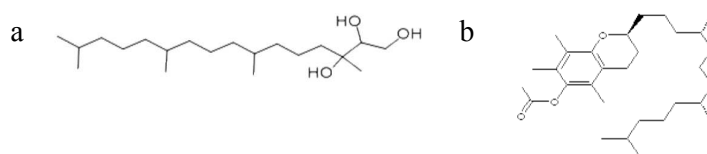
The unique nature of the positronium probe and its specific interaction with matter can provide information in this domain that is otherwise unattainable with conventional methods. In recent years, positron annihilation lifetime spectroscopy (PALS) has demonstrated its utility as a molecular probe in soft condensed matter systems. PALS has been used to determine the critical micelle concentration (CMC) of surfactants;^[23-26] to distinguish transformations in micellar geometry^[27-32] as well as phase transitions in lyotropic liquid crystalline systems^[33-36] ^[37, 38] and lipid bilayers. ^[37, 39-45] The decay of radioactive nuclei such as ²²Na leads to the generation of orthopositroniums (*o*Ps); where *o*Ps lifetime (τ_{oPs}) may be considered an active probe of both intrinsic packing and chain mobility.^[42, 46] PALS techniques however, have not been broadly utilised by the amphiphile self-assembly community as the structural diversity displayed by amphiphiles, inherent heterogeneity and dynamic fluidity of these systems add complexity to the positron decay paths and data analysis.

We have previously established that the *o*Ps lifetimes of some phospholipid bilayer structures distinguishes the effects of morphology and nanostructure. ^[37] In the current work therefore we extend this hypothesis to include other structures and lipids of biophysical and/or pharmaceutical relevance. Specifically we have systematically examined the PALS response across the $Q_2 \rightarrow H_2 \rightarrow L_2$ phase transition boundaries of cubosome dispersions prepared from phytantriol (3,7,11,15-tetramethyl-1,2,3-hexadecane-triol, Figure 1a). This lipid is of interest in the cosmetics industry to improve moisture retention and promote skin penetration,^[9, 47, 48] and has potential in transdermal drug delivery.^[49] The phase behaviour of this lipid is well characterised ^[50, 51] (Figure S1) and we have previously examined the PALS response in the non-dispersed lyotropic liquid crystalline system.^[33] To investigate the sensitivity of the PALS parameters to encapsulated compounds we have further examined the ternary phytantriol-vitamin E acetate (VitEA)-water system wherein VitEA has been used as a model (hydrophobic) drug (Figure 1b).

Materials and Methods

Materials

Phytantriol (3,7,11,15-tetramethylhexadecane-1,2,3-triol) (>95 % purity) was a gift from DSM (Basel, Switzerland) and was used without further purification. Vitamin E acetate (VitEA) was purchased from Sigma Aldrich Chemie (Steinhiem, Germany). Pluronic[®] F127 was purchased from BASF (Florham Park, NJ). Water was purified for this study using a MilliQ system (Millipore, Sydney, Australia). The ²²Na source used in PALS measurements was purchased as an aqueous solution of NaCl from Perkin Elmer (Waltham, USA). Mylar sheets of 2.54 μm thickness were used to seal the source. The calibration standard silver behenate ($a = 58.38 \text{ \AA}$) for small angle x-ray scattering (SAXS) experiments was obtained from Sigma Aldrich (St Louis, USA).



c

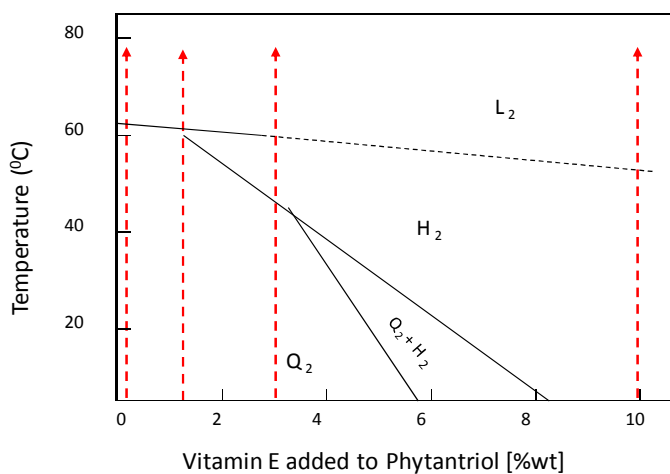


Figure 1 a): Structure of phytantriol (3,7,11,15-tetramethylhexadecane-1,2,3-triol) and b) vitamin E acetate c) Partial phase diagram of phytantriol-VitEA-water dispersions (re-drawn from Dong *et al.*[11]) PALS and SAXS data were collected at VitEA ratios of 1, 3, and 10 %w/w (total lipid) over the temperature range 0-55°C (hashed red lines).

Preparation of lyotropic liquid crystalline dispersions

Phytantriol and vitamin E acetate (1, 3 and 10% w/w of total lipid content) were weighed into a glass vial in sufficient quantity to produce a lipid content of 30% (w/w) in the final dispersion. The lipid content was optimised to realise PALS measurements with good signal to noise ratios. The lipids were mixed on rollers at 30°C for at least two days. MilliQ water containing Pluronic[®] F127 (1% w/w) was then added to the homogenous lipid mixture. The samples were immediately dispersed via ultrasonication (Misonix, USA). Samples were equilibrated for approximately two weeks at 30°C before characterisation.

Positron annihilation lifetime spectroscopy (PALS)

When an energetic positron is injected into a sample it undergoes a series of inelastic collisions with its surroundings to arrive at thermal equilibrium (10^{-12} s). The thermalised positrons may undergo free annihilation with electrons within the material at a rate that depends on the electron density of the medium with lifetimes of typically 100-500 ps, or form a bound positron-electron pair (*positronium* (Ps)). Of most relevance to this study are the *ortho*-positronium (*o*Ps) as these preferentially localise in the free volume pockets in the material. In vacuum, *o*Ps has a relatively long lifetime of 142 ns, whereas in a medium the *o*Ps undergoes pick-off annihilation with an electron during collision with molecules in the cavity wall in which it is localized. The pick-off process reduces the lifetime of *o*Ps down to a few nanoseconds. *o*Ps accumulates in regions of low electron density and *o*Ps lifetimes (τ) and intensities (I_{oPs}) have been associated with the size of free volume sites and the probability of formation or the number of free volume elements present.

Positron annihilation lifetime spectroscopy measurements were performed as a function of temperature, between 10-55°C. The samples were loaded into a custom-designed liquid sample holder that has been described elsewhere[52]. The radioactive ²²Na source (30 μ Ci) was encased in Mylar, and was washed with absolute ethanol and air dried between samples. A minimum of five spectra each with 5×10^5 counts were collected at each temperature and composition. Details of the PALS fitting procedure are provided elsewhere. [33, 53] Raw PALS data was analysed using both LT9 and Pascual fitting software programs using a four component fit. As water comprises 70% (w/w) of the dispersed systems, separation of the organic and aqueous contributions to *o*Ps was required so that trends in the organic region could be distinguished. The components in increasing order of longevity correspond to

annihilation of para-positroniums (τ_1), direct annihilation of free positrons (τ_2) and the annihilation of ortho-positroniums in the aqueous and organic phases (τ_3 , τ_4 respectively). Each lifetime has a corresponding intensity I that is related to the concentration of void sites in the medium. For the fitting procedure, τ_1 was fixed at 0.125 ns, with the lifetime for water (τ_3) fixed at 1.8 ns [54] with a source correction of 1.857 ns and 3.52% also applied. Table 1 lists the initial refinement parameters used for the PALS fitting procedure.

Table 1: Initial parameter inputs for PALS spectral analysis

<i>Component</i>	<i>Lifetime (ns)</i>	<i>Intensity (%)</i>
<i>pPs annihilation</i>	0.125 (fixed)	-
<i>Direct annihilation</i>	0.400 (free)	-
<i>oPs annihilation (water)</i>	1.80 (fixed)	-
<i>oPs annihilation (lipid)</i>	3.00 (free)	-
Source correction	1.857	3.52

Small angle X-ray scattering (SAXS)

Small angle X-ray scattering of samples measured for PALS was used to identify the phase and transition temperatures for each dispersed liquid crystalline system. The SAXS measurements were performed at the Australian Synchrotron SAXS/WAXS Beamline. Samples were loaded into glass capillaries of 1.5 mm diameter (Charles Supper, USA) and inserted into a custom built multi-capillary holder. The temperature of the sample holder was maintained by a Peltier controller to an accuracy of $\pm 0.1^\circ\text{C}$ (Linkam LTS 120 with PE04 controller). Samples were equilibrated at each temperature for five min before measurement using a one sec exposure.

Dynamic light scattering (DLS)

DLS experiments were performed on a Zetasizer Nano ZS (Malvern, Worcestershire, UK). The samples were diluted with MilliQ water and placed into a plastic micro volume cuvette (Sarstedt, Germany). Measurements were performed at 30 °C and samples were allowed to equilibrate for three min. Triplicate measurements with a minimum of 12 runs were performed.

Cryogenic transmission electron microscopy (Cryo-TEM)

Samples were diluted with MilliQ water (1:20 v/v) for cryo-TEM measurements. Approximately 4 μl of the sample was placed onto a 300 mesh copper TEM grid coated with a lacy carbon film (ProSciTech, Australia) that was then rendered hydrophilic via glow discharge. Excess sample was removed by manual blotting with filter paper and the sample

grid was vitrified by being rapidly plunged into liquid ethane (approximately -180°C). The grids were stored in liquid nitrogen before being transferred into a Gatan 626-DH Cryo-holder, where samples were maintained at -180°C during imaging. Cryo-TEM imaging was performed on a FEI Tecnai 12 TEM (120 kV) with a MegaView III CCD camera and AnalySis imaging software (Olympus Soft Imaging Solutions).

Results

Characterisation of dispersion structure and particle size distribution

Table 2 contains the particle size and polydispersity index data at 30°C for the four dispersed systems containing 0, 1, 3 and 10 wt/wt% VitEA. The particle sizes obtained from DLS agreed well with visual observations from cryo-TEM and range from ~ 200 - 290 nm with decreasing VitEA composition (Figure 2). There is a transition from predominantly cubic nanostructure (cubosomes) at low VitEA content to mainly hexagonal architectures (hexosomes) at higher doping concentrations that is consistent with the scattering behaviour observed from SAXS (Figure 2 d and Table 3). The inverse bicontinuous cubic phase present in these dispersions has the space group $\text{Pn}3\text{m}$ (Figure S2 Supplementary Information).

Table 2 - Particle size (nm) and polydispersity index (PDI) for the dispersed systems at 30°C .

Vitamin E acetate content (% w/w)	Particle size (nm)	Polydispersity index (PDI)
0	288.1 ± 11.1	0.22 ± 0.03
1	220.0 ± 4.8	0.42 ± 0.02
3	201.1 ± 3.4	0.33 ± 0.01
10	194.8 ± 5.1	0.31 ± 0.02

Table 3 - Transition temperatures ($^{\circ}\text{C}$) for the dispersed systems as measured by SAXS.

Vitamin E acetate content (% w/w)	$\text{Q}_{2 \text{ Pn}3\text{m}} \rightarrow \text{Q}_{2 \text{ Pn}3\text{m}} + \text{H}_2$	$\text{Q}_{2 \text{ Pn}3\text{m}} + \text{H}_2 \rightarrow \text{H}_2$	$\text{H}_2 \rightarrow \text{L}_2$
0	44.7 – 49.4	54.3 – 58.9	58.9 – 66.3 (65) *
1	39.7 – 42.5	48.4 – 50.8	59.8 – 67.0 (65) *
3	-	35.4 – 38.5 (45) *	59.0 – 67.0 (65) *
10	-	-	52.0 – 55.3 (50) *

* [11]

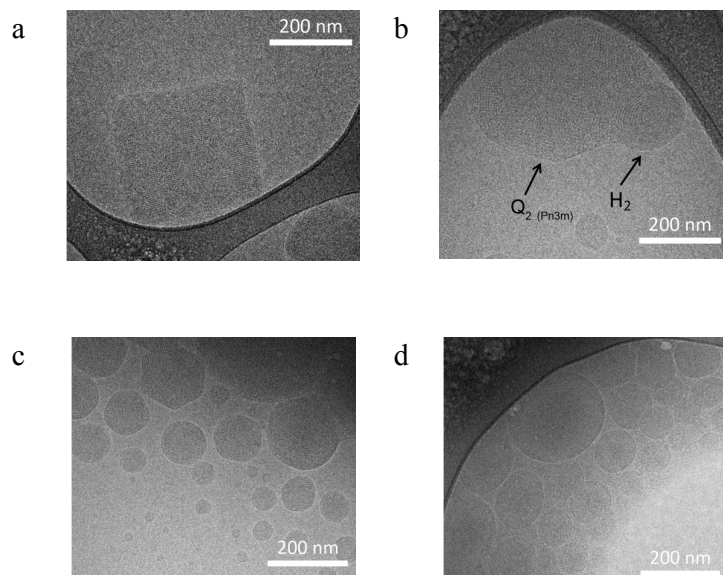


Figure 2: Cryo-TEM images of a) phytantriol cubosomes, b) phytantriol with 1% (w/w) VitEA showing majority cubosomes with some hexosomes also present, c) and d) hexosomes observed in phytantriol with 3% and 10% (w/w) vitamin E acetate, respectively.

PALS results

Figure 3 presents the *o*Ps lifetime behaviour in the organic region (τ_4) as a function of temperature for the dispersed phytantriol/water systems with 0%, 1%, 3% and 10% (w/w) VitEA, respectively. For the dispersed system with no VitEA, a sharp increase in *o*Ps lifetime was observed between 45-50°C (Figure 3A), which corresponds to the $Q_2 \text{ Pn3m} \rightarrow H_2$ transition as identified from SAXS (Table 3). At temperatures below the phase transition temperature, τ_4 was relatively invariant with a value of $\tau_4 \sim 2.2$ ns; increasing to $\tau_4 \sim 4$ ns upon transition to the H_2 phase above 45-50 °C. The magnitude of this increase was approximately 1.8 ns, which is significantly greater than the increase observed for the non-colloidal mesophase (0.2 ns) previously measured.[33] For the dispersed colloidal systems containing VitEA a more gradual increase in *o*Ps lifetime with temperature (from 3.8 ns to 4.0 ns) is observed (Figure 3B-D). This trend is similar to that observed in the bulk phytantriol/water systems in previous studies. [33]

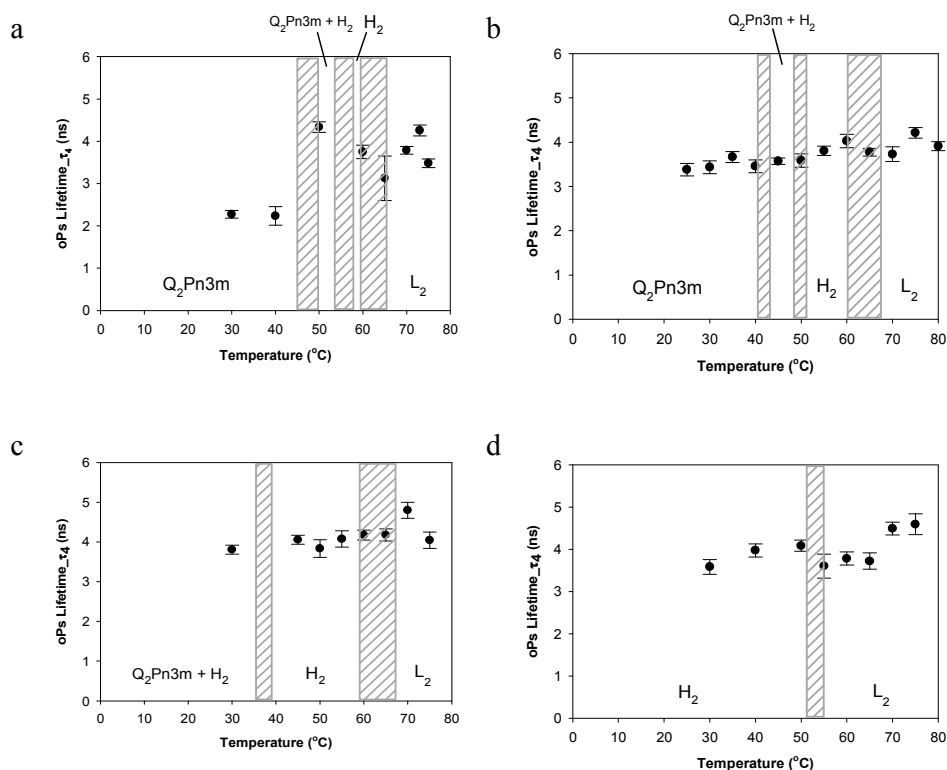


Figure 3: oPs lifetime in the organic region (τ_4) for the dispersed colloidal phytantriol/water systems with increasing concentration of vitamin E acetate. A) 0%, B) 1%, C) 3% and D) 10% (w/w) VitEA. Phase transitions as measured by SAXS are marked in the hashed regions.

There was a sharp decrease in oPs intensity with temperature for the organic region (I_4) at the Q₂ Pn_{3m} → H₂ phase boundary for the dispersed colloidal phytantriol/water system (Figure 4A) with I_4 decreasing from 20% to approximately 7%. However, the incorporation of VitEA up to 10 % w/w did not produce any significant change in I_4 which remained invariant at approximately 7% (Figure 4B-D). For the dispersed colloidal system with no vitamin E acetate, the oPs intensity in the aqueous region (I_3) increased from approximately 1% in the Q₂ Pn_{3m} phase to 15% in the H₂ phase (Figure 5A). As with the values of I_4 in the organic region, the addition of VitEA had little effect upon the intensity values as a function of temperature. At 1% (w/w) the I_3 is ~ 7% irrespective of temperature, which approximately doubled at 3 and 10% VitEA to I_3 is ~15% (Figure 5B).

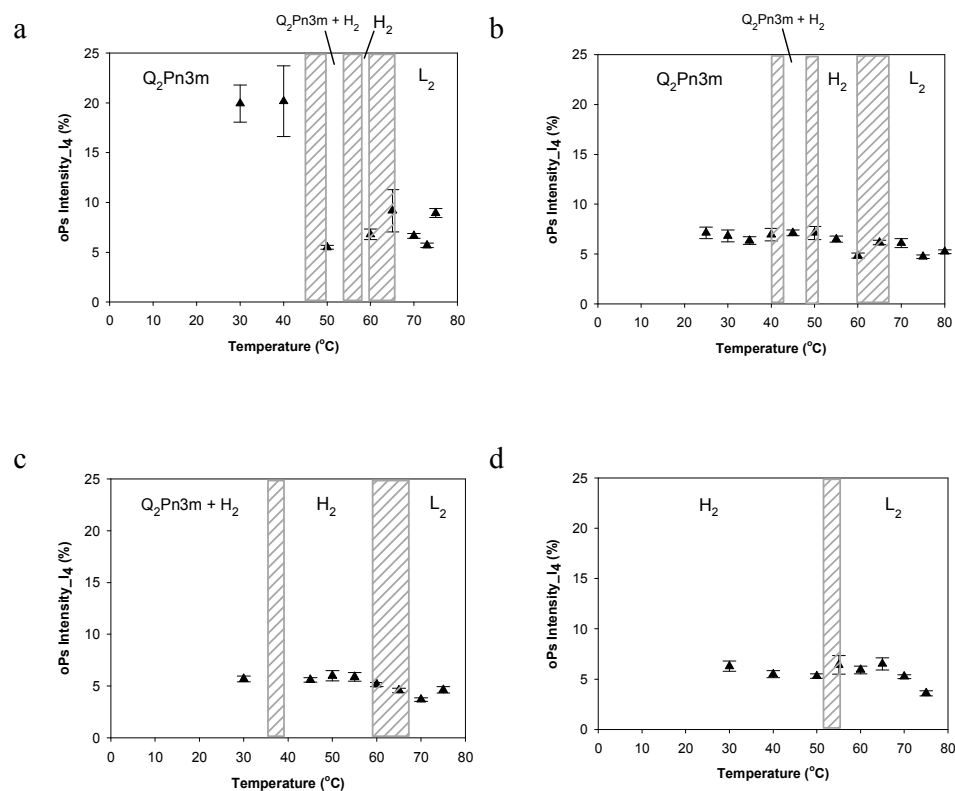


Figure 4: *oPs* intensity in the organic region (I_4) for the dispersed colloidal phytantriol/water systems with increasing concentration of vitamin E acetate. A) 0%, B) 1%, C) 3% and D) 10% (w/w) VitEA. Phase transitions as measured by SAXS are marked in the hashed regions.

Discussion

It is now widely recognised that molecular mobility is determined by the thermodynamic state as well as the local free volume which exists between molecules in soft matter due to irregular packing, density fluctuations and topological constraints. The unique nature of the positronium probe and its specific interaction with matter can provide information in this domain that is otherwise unattainable with conventional methods. There are diverse regions of varying electron density wherein *oPs* may annihilate. We have previously determined with the data analysis using PAscuAl that the *oPs* does not annihilate in the water phase, [34] so it was deduced that *oPs* annihilation occurs in the hydrophobic domain, consistent with previous observations.[33, 53] Duplatre[55] have postulated that *oPs* forms in the aqueous region. These authors also propose that *oPs* diffuses to, and annihilates in the hydrocarbon domains, which has implications for macroscopic properties such as viscosity and diffusion.[56-58]

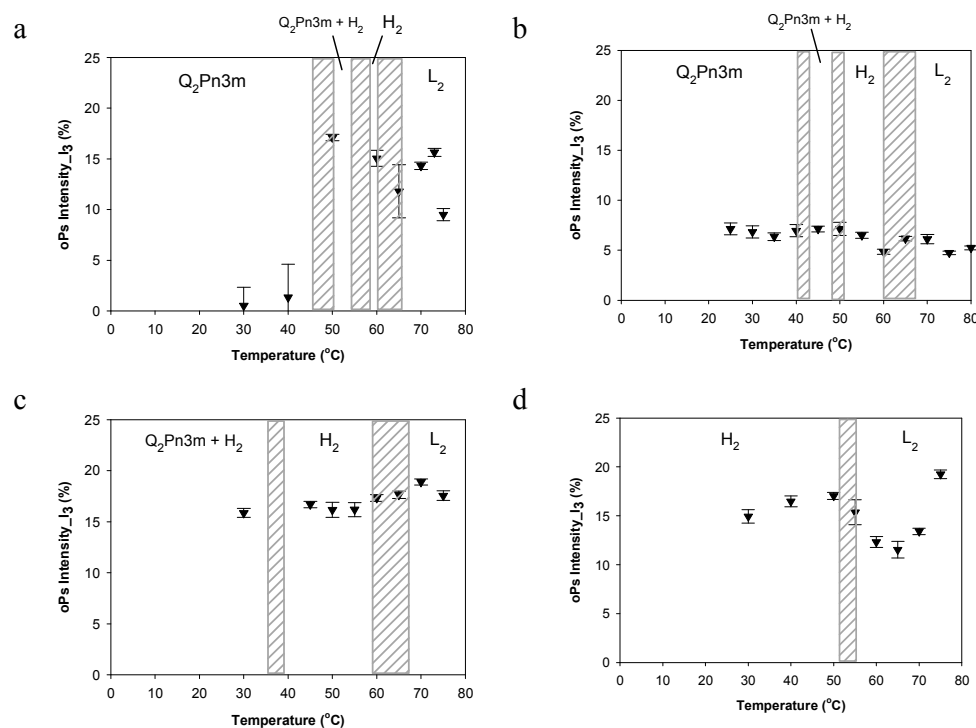


Figure 5: oPs intensity in the aqueous region (I_3) for the dispersed colloidal phytantriol/water systems with increasing concentration of vitamin E acetate. A) 0%, B) 1%, C) 3% and D) 10% (w/w) VitEA. Phase transitions as measured by SAXS are marked in the hashed regions.

There are relatively few studies of the application of PALS to lyotropic liquid crystalline amphiphile systems. Previously much of this work has focussed upon the measurement of micellar growth and geometry in the Type I [1] normal phases for charged amphiphiles[29, 35] such as CTAB,[27, 59] and SDS.[25, 60] The PALS signature for dispersions of self-assembled colloidal materials has only recently been reported for the lamellar phase (liposomes); [45, 61, 62] [63] with very few studies of Type II [1] inverse architectures such as Q_2 and H_2 phases, which are the subject of increasing interest for nanotechnology and biomedical applications [4, 20, 64] The current work therefore constitutes the first report of PALS for the characterisation of dispersed lyotropic liquid crystalline particles with two- and three- dimensional internal order. For many applications dispersions such as cubosomes and hexosomes are preferred since these possess the same nanostructure as the parent phase, though have much lower viscosity (by a factor of 10^8) and higher surface area; to enable ease of formulation for increased payload.

Effect of lyotropic liquid crystalline nanostructure on the PALS parameters of colloidal dispersions of the phytantriol-water system

The phase behaviour of the phytantriol-water system is well characterised and is re-drawn in Figure S1.[50, 51] The sequence of phases formed is the result of the interplay between local and global constraints in the system. The former influences the local interfacial curvature and is a factor of the effective molecular shape of the amphiphile as described by the critical packing parameter (CPP).[3] Of particular interest to this study is the fact that at compositions greater than *c.a* 30 w/w % water, phytantriol undergoes a $Q_2 \text{ Pn}_{3m} \rightarrow H_2 \rightarrow L_2$ phase transition with increasing temperature that is thermodynamically stable in excess water. The stability at high dilution is of particular importance for drug delivery, as this provides the necessary condition required for dispersion as cubosomes and hexosomes.[65, 66] The phase transitions of the lyotropic liquid crystalline colloidal dispersions are analogous to the non-colloidal mesophase transitions.[11]

The sensitivity of PALS to internal nanostructure has been investigated through comparison of ρ Ps and $I_{\rho\text{Ps}}$ of both the colloidal dispersions (cubosomes and hexosomes) and “bulk” mesophases.[11] Nanostructure has been shown to be an important parameter in the release kinetics for drug delivery (*i.e.* intravenous vs depot) and several workers have shown that the nanostructure of the phase impacts upon the release profile of the drug.[20, 67, 68] Dong *et al.* [33] have recently characterized the PALS signature of the $Q_2 \text{ Pn}_{3m} \rightarrow H_2 \rightarrow L_2$ transition sequence for the non-colloidal phytantriol-water system; specifically characteristic lifetimes were observed for each mesophase where the mobility of the hydrocarbon chains and PALS lifetimes (τ_4) decreased in the order L_2 ($\tau_4 \sim 3.1$ ns) > H_2 ($\tau_4 \sim 3.0$ ns) > $Q_2 \text{ Pn}_{3m}$ ($\tau_4 \sim 2.8$ ns). These lifetime signatures are arrived at regardless of the route by which the transition was affected (*i.e.* temperature vs composition). Characteristic lifetimes with a similar sequence or “ranking” were observed for the analogous dispersions in the present work; *viz* L_2 ($\tau_4 \sim 4$ ns) \sim H_2 ($\tau_4 \sim 4$ ns) > $Q_2 \text{ Pn}_{3m}$ ($\tau_4 \sim 2.2$ ns). Hence a discontinuity in PALS signature is observed across the $Q_2 \text{ Pn}_{3m} \rightarrow H_2$ phase transition in cubosomes arising as a function of either increasing temperature or composition. The values of τ_4 are higher overall in the aqueous colloidal dispersions which is similar to what was previously observed between the “bulk” lamellar phase and its colloidal dispersions (liposomes).[69] Based upon the PALS lifetimes it may be anticipated that the diffusion of hydrophilic moieties from the colloidal dispersions would be more rapid than the “bulk” mesophase, which is reasonable given the greater surface area of these as nanoparticles.

Eldrup and co-workers[70] have established a quantitative semi-empirical relationship correlating the *o*Ps lifetimes with the radius (R) of a spherical trap where annihilation occurs:

$$\tau = \frac{1}{2} \left[1 - \frac{R}{(R+C)} + \frac{1}{2} \pi \sin\left(\frac{2\pi R}{R+C}\right) \right]^{-1} \quad \text{where } C = 0.166 \text{ nm}$$

We have used this model to estimate the dynamic free volume sizes within these mesophases so that we may obtain a handle on the mobility of the lipid chains and their ability to accommodate a diffusing entity (i.e., *o*Ps pushing aside surrounding molecules). Table 4 compares the void sizes and volume for the “bulk” mesophase[33] and the colloidal dispersions examined in this study. The molecular proximity at the annihilation site, *d* increases in the order $Q_2 \text{ Pn3m} < H_2 < L_2$ in the “bulk” systems; whereas for the corresponding dispersions $Q_2 \text{ Pn3m} < H_2 \sim L_2$. The $Q_2 \text{ Pn3m}$ has the shortest lifetime in both the non-colloidal and dispersed systems which is interpreted as the bicontinuous cubic phase having the tightest molecular packing (highest electron density) at the annihilation site (Table 4).[33] The increase in τ_4 for the $Q_2 \text{ Pn3m} \rightarrow H_2$ transition for both the “bulk” mesophase and colloidal dispersions is consistent with greater conformational disorder and splay of the hydrocarbon chain at higher temperatures. Interestingly there is no significant change in *o*Ps lifetime for the $H_2 \rightarrow L_2$ transition in either the “bulk” mesophase or the colloidal dispersions, suggesting that the hydrocarbon chain mobility is similar in these phases. As the lipid chains comprise a network continuum between the rod-like and spherical micelles in the H_2 and L_2 phases the similarities in PALS parameters is reasonable. In other words, the dynamic chain packing at higher temperatures and in the L_2 and H_2 phases is qualitatively less “viscous.” Rheological comparisons of the “bulk” phases support these observations whereby the L_2 phase is more fluid than the H_2 phase, with the $Q_2 \text{ Pn3m}$ phase the most rigid phase. [71, 72]

Table 4: Calculated void sizes and void volume of the bulk mesophases and colloidal dispersions (no VitEA)

Form	Phase	τ_4 (ns)	<i>d</i> (Å)	V_{void} (nm ³)
Bulk [33]	L_2	3.1	7.46	0.22
	H_2	3.0	7.31	0.20
	$Q_2 \text{ Pn3m}$	2.9	7.12	0.19
Dispersion	L_2	4.0	8.4	0.32
	H_2	4.0	8.4	0.32
	$Q_2 \text{ Pn3m}$	2.2	6.0	0.12

The magnitude of change in τ_4 for the $Q_2 \text{ Pn3m} \rightarrow H_2$ transition is somewhat larger in the dispersed colloidal system (~1.8 ns) than the corresponding bulk system (0.2 ns). This result may suggest that there is a larger difference in hydrocarbon chain packing and mobility

between the two phases when the system is dispersed; however is more likely due to differences in data analysis. For the “bulk” mesophase system the data was deconvoluted into only three components, with the last component corresponding to an averaged *o*Ps lifetime value that has contributions from both the organic (τ_4) and aqueous regions (τ_3). In the present study, the *o*Ps annihilation has been separated into organic and aqueous contributions which are required to account for the significantly greater overall water content. It is unlikely that the difference in water content between the “bulk” and dispersed lyotropic liquid crystalline systems had any direct effect on the magnitude of increase in τ_4 across the Q_2 $P_{n3m} \rightarrow H_2$ phase transition. The higher overall water content in the dispersed colloidal system is only anticipated to affect the observed *o*Ps intensity, while the *o*Ps lifetime of water should remain unchanged (1.8 ns) in both the “bulk” mesophase and dispersed colloidal systems. The PALS data for the current dispersed colloidal system was re-analysed with three components, and confirms a similar difference (0.2 ns) in the magnitude of τ_4 across the Q_2 $P_{n3m} \rightarrow H_2$ transition as that observed in the “bulk” lyotropic liquid crystalline system. This highlights some of the difficulties in comparing PALS data across the existing literature.[52]

Effect of vitamin E acetate on the PALS parameters of colloidal dispersions

VitEA is lipophilic and will most likely partition into the hydrophobic regions of the lipid bilayer to qualitatively increase the volume of the hydrophobic footprint of the molecule and so impart an increased negative interfacial curvature on the system. Dong and co-workers[51] have shown that the addition of small amounts of VitEA to the phytantriol-water system not only preferences inverse type mesophases as manifest by the disappearance of the lamellar phase but also acts to suppress the Q_2 $P_{n3m} \rightarrow H_2 \rightarrow L_2$ transition temperatures. With increased addition of VitEA there is a corresponding broadening of the temperature range of the $Q_2 + H_2$ co-existence region.[11]

In the dispersed colloidal systems, VitEA was added at concentrations of 1%, 3% and 10% (w/w) of the total lipid content. A gradual increase in *o*Ps lifetime was observed as a function of temperature that is unlike the abrupt increase in τ_4 observed for neat phytantriol-water systems. In other words the addition of small amounts of VitEA did not significantly alter the *o*Ps lifetimes, suggesting preferential partitioning of the molecule in the hydrophobic region as expected. This is attributed to the existence of mixed populations of cubosomes and

hexosomes at all doping levels (Figure 2), giving rise to $\tau \sim 3.5$ ns that is most likely an average lifetime value of the two mesophases.

Based upon the PALS lifetimes it may be anticipated that the diffusion of (hydrophilic) drugs from the H_2 phase would be enhanced over the Q_2 (cubosomes) (Table 3). However the correlation between diffusion-dependent transport and hydrocarbon chain mobility is more complicated, with the release rate also affected by the nature of the drug e.g hydrodynamic radius, hydrogen bonding, hydrophilicity, and solubility, as well as host matrix chemical and mesophase structure. Boyd *et al.* have demonstrated slower release rates of some model hydrophilic and hydrophobic drugs from the non-dispersed lyotropic H_2 phase relative to the Q_2 phase.[12] This was attributed to differences between the geometry of the aqueous domains that provide the principal route for drug release for both hydrophobic and hydrophilic drugs. In the case of the Q_2 phase, this consists of two non-interpenetrating, congruent water networks that are likely open to the outside aqueous media.[1, 73, 74] In contrast, the aqueous compartments in the H_2 phase are closed columnar tubes and it is anticipated that the release of drugs would require perturbations of this structure for diffusion. It is also generally believed that the rate limiting factor for controlling drug release is the diffusion through the aqueous domains rather than the lipid regions.

Effect of Pluronic® F127 on the PALS parameters

Cubosomes and hexosomes are submicron colloidal dispersions commonly prepared using non-ionic lipids such as monoolein[5, 75-77] and phytantriol.[78] To prevent flocculation and phase separation after dispersion, non-ionic block copolymers such as Pluronic F127 (abbreviated to 'F127') are used as steric stabilisers [8] [79] that can further impart 'stealth' functionality to reduce premature clearance of such nanoparticles during *in vivo* circulation.[80] These comprise triblock polyethylene oxide - polypropylene oxide - polyethylene oxide copolymers (PEO-PPO-PEO) with general formula $(CH_3)(CH_2)_x-10(CH_2CH_2O)_nH$. These adsorb to the external and internal cubo(hexo)some surface, with partitioning into the lipid bilayer of the mesophase to provide stabilisation via interparticle repulsion. Gustafsson *et al.* [74] have demonstrated that incorporation of F127 into the bilayer occurs at sufficiently high concentrations and has the effect of changing the nanostructure of monoolein-based cubosomes with a transition from the $Q_2 Pn3m \rightarrow Q_2 Im3m$; which is not observed for phytantriol-based cubosomes. Tilley *et al.* suggest that the association of F127 is a function of particle internal nanostructure as well as lipid type. They

propose that the hydrophobic polypropylene oxide (PPO) portion acts to anchor the stabiliser in the bilayer in monoolein-based cubosomes, thereby promoting a change in nanostructure; whereas for phytantriol-based cubosomes the F127 adsorbs externally to the bilayer.[73] In general it is believed that the hydrophilic polyethylene oxide (PEO) portion of the stabiliser extends into the surrounding continuous phase to provide a steric barrier against aggregation. Previous studies by Li et al. [81] proposed that the Pluronic stabilisers exhibited two different structural conformations on polystyrene colloids. At high surface concentrations, the PEO chains of the stabiliser are extended into the continuous phase in the “brush” conformation. The ‘mushroom’ conformation exists when there is low surface concentration of the stabiliser.

The F127 concentration was not varied in this study and was maintained at 1 w/w % for all dispersion formulations. Its effect upon the PALS parameters is therefore difficult to deconvolute. The hydrophilicity of the PEO chains and their proposed distribution at the cubo(hexo)some surface is unlikely to affect the ρ Ps lifetime in the organic region. The lifetime in the aqueous region may be marginally affected. The interaction between the hydrophilic PEO chains and bulk water may result in the presence of ‘bound’ water near the particle surface and cause a deviation away from the value of 1.8 ns for τ_3 . Whilst we acknowledge that this may be a factor, the effect of bound water versus bulk water on the PALS parameters cannot be discriminated but this effect will be very small as a consequence of the large volume of bulk water. Similarly the incorporation into the mesophase bilayer of the PPO segments of the di-block copolymer cannot be explicitly separated from that of VitEA that is also expected to be incorporated in this region.

Conclusions

We have examined the information provided by PALS to probe dynamic processes in lyotropic liquid crystalline colloidal dispersions of interest in the pharmaceutical, food and personal care industries. The PALS lifetime signature is sensitive to changes in the molecular packing and mobility (i.e permeability) in these systems that have been induced by changes in temperature, matrix composition (addition of VitEA) and water content (phase behaviour). Characteristic PALS lifetimes for L_2 ($\tau_4 \sim 4$ ns) \sim H_2 ($\tau_4 \sim 4$ ns) $>$ Q_2 Pn3m ($\tau_4 \sim 2.2$ ns) were observed, with the dynamic free volume sizes within these mesophases following a similar trend *viz* L_2 ($\tau_4 \sim 0.32$ nm³) \sim H_2 $>$ Q_2 Pn3m ($\tau_4 \sim 0.12$ nm³). As the hydrocarbon packing

comprises the network through which small (liposoluble) species must diffuse, tailoring the lyotropic liquid crystalline phases offers the potential to control the release kinetics.

Electronic Supplementary Information – ESI is available for this article free of charge, containing partial phase diagrams and Small Angle X-ray scattering (SAXS) data.

Acknowledgement This research was supported under the Australian Research Council's (ARC) Discovery Projects funding scheme (project number DP0667189). This research was undertaken on the SAXS/WAXS beamline at the Australian Synchrotron, Victoria, Australia. AD thanks the Faculty of Pharmacy and Pharmaceutical Sciences for a postgraduate scholarship to conduct these studies, and thanks CSIRO for a top up scholarship. CJD was the recipient of an ARC Federation Fellowship. BJB is the recipient of an ARC Future Fellowship.

References

- [1] Hyde ST, Andersson S, Larsson K, Blume Z, Landh T, Lidin S, et al. The language of shape: Elsevier Science B.V.; 1997.
- [2] Tanford C. The Hydrophobic Effect: Formation of Micelles and Biological Membranes. New York: John Wiley and Sons; 1973.
- [3] Israelachvili J, N., Mitchell DJ, Ninham BW. J Chem Soc Faraday Trans II. 1976;72:1525-68.
- [4] Drummond CJ, Fong C. Surfactant self-assembly objects as novel drug delivery vehicles. Current Opinion in Colloid & Interface Science 1999;4:449-56.
- [5] Yaghmur A, Glatter O. Characterization and potential applications of nanostructured aqueous dispersions. Advances in Colloid and Interface Science. 2009;147-148:333-42.
- [6] Mulet X, Kennedy DF, Conn CE, Hawley A, Drummond CJ. High throughput preparation and characterisation of amphiphilic nanostructured nanoparticulate drug delivery vehicles. International Journal of Pharmaceutics. 2010;395:290-7.
- [7] Engstrom S. Drug delivery from cubic and other lipid/water phases. Lipid technology. 1990;2:42-5.
- [8] Engstrom S, Lindman B, Larsson K. Method of preparing controlled release preparations for biologically active materials and resulting compositions. 1992;US 5151272.
- [9] Ericsson B, Eriksson PO, Loeffroth JE, Engstroem S, Ferring AB, Malmoe S. Cubic phases as delivery systems for peptide drugs. ACS Symposium series 469. 1991:251 - 65.
- [10] Boyd BJ, Whittaker D, Khoo SM, Davey G. Hexosomes formed from glycerate surfactants-Formulation as a colloidal carrier for irinotecan. International Journal of Pharmaceutics. 2006;318:154-62.
- [11] Dong YD, Larson I, Hanley T, Boyd BJ. Bulk and Dispersed Aqueous Phase Behavior of Phytantriol: Effect of Vitamin E Acetate and F127 Polymer on Liquid Crystal Nanostructure. Langmuir. 2006;22:9512-8.
- [12] Boyd BJ, Whittaker DV, Khoo S-M, Davey G. Lyotropic liquid crystalline phases formed from glycerate surfactants as sustained release drug delivery systems. International Journal of Pharmaceutics. 2006;309:218-26.
- [13] Mulet X, Boyd BJ, Drummond CJ. Advances in drug delivery and medical imaging using colloidal lyotropic liquid crystalline dispersions. Journal of Colloid and Interface Science. 2013;393:1-20.
- [14] Amar-Yuli I, Libster D, Aserin A, Garti N. Solubilization of Food Bioactives Within Lyotropic Liquid Crystalline Mesophases. Current Opinion in Colloid & Interface Science. 2009;14:21-32.
- [15] Desai KGH, Park HJ. Recent Developments in Microencapsulation of Food Ingredients. Drying Technology. 2005;23:1361-94.
- [16] Larsson K. Lyotropic Liquid Crystals and Their Dispersions Relevant in Foods. Current Opinion in Colloid & Interface Science. 2009;14:16-20.
- [17] Taylor TM, Davidson PM, Bruce BD, Weiss J. Liposomal Nanocapsules in Food Science and Agriculture. Critical Reviews in Food Science and Nutrition. 2005;45:587-605.
- [18] Garti N, Libster, D., Aserin, A. Lipid polymorphism in lyotropic liquid crystals for triggered release of bioactives. Food and Function. 2012;3:700-13.
- [19] Du JD, Liu Q, Salenting S, Ngyuen TH, Boyd BJ. A novel approach to enhance the mucoadhesion of lipid drug nanocarriers for improved drug delivery to the buccal mucosa International Journal of Pharmaceutics. 2014;471:358-65.
- [20] Fong C, Le T, Drummond CJ. Lyotropic liquid crystal engineering-ordered nanostructured small molecule amphiphile self-assembly materials by design. Chemical Society Reviews. 2012;41:1297-322.

- [21] Lee K W Y, Ngyuen T-H, Hanley T, Boyd B J. Nanostructure of liquid crystalline matrix determines in vitro sustained release and in vivo oral absorption kinetics for hydrophilic drugs. *International Journal of Pharmaceutics*. 2009;365:190-9.
- [22] Phan S, Fong W-K, Kirby N, Hanley T, Boyd B J. Evaluating the link between self assembled mesophase structure and drug release. *International Journal of Pharmaceutics*. 2011;421:176-82.
- [23] Bockstahl F, Duplatre G. A new method to determine micellar aggregation numbers: positron annihilation lifetime spectroscopy. *Phys Chem Chem Phys*. 2000;2:1-5.
- [24] Bockstahl F, Duplatre G. Quantitative determination of a sodium dodecylsulfate micellar radius through positron annihilation lifetime spectroscopy. *Phys Chem Chem Phys*. 1999;1:2767-72.
- [25] Bockstahl F, Pachoud E, Duplatre G, Billard I. Size of sodium dodecyl sulphate micelles in aqueous NaCl solutions as studied by positron annihilation lifetime spectroscopy. *Chemical Physics*. 2000;256:307-13.
- [26] Duplatre G, Ferreira Marques MF, da Graca Miguel M. Size of Sodium Dodecyl Sulfate Micelles in Aqueous Solutions as Studied by Positron Annihilation Lifetime Spectroscopy. *Journal of Physical Chemistry*. 1996;100:16608-12.
- [27] Choudhury SR, Yadav R, Maitra AN, Jain PC. Structural transformations in CTAB aggregated systems investigated by positron lifetime spectroscopy 1. Binary systems. *Colloids and Surfaces A: Physicochemical and Engineering Aspects*. 1994;82:49-58.
- [28] Choudhury SR, Yadav R, Maitra A. N., Jain P. C. . I. Positron annihilation studies in ctav reversed micellar systems. In: Dorikens-Vanpraet L, Dorikens M, Segers D, editors. *ICPA-8*. Gent Belgium: World Scientific; 29 August-3 September 1989. p. 818-20.
- [29] Jain PC. Positron annihilation spectroscopy and micellar systems. *Advances in Colloid and Interface Science*. 1995;54:17-54.
- [30] Yadav R, Singh KC, Choudhury SR, Jain PC. Detection of bicontinuous phase in some reverse micellar systems by positron lifetime spectroscopy. *Phys Stat Sol C*. 2007;4:3785-8.
- [31] Jean YC, Ache HJ. Positronium reactions in micellar systems. *J Am Chem Soc*. 1977;99:7504-9.
- [32] Jean Y-C, Ache HJ. Determination of critical micelle concentrations in micellar and reversed micellar systems by positron annihilation techniques. *Journal of the American Chemical Society*. 1978;100:984-5.
- [33] Dong AW, Pascual-Izarra P, Pas SJ, Hill AJ, Boyd B J, Drummond CJ. Positron Annihilation Lifetime Spectroscopy (PALS) as a Characterisation Technique for Nanostructured Self-Assembled Amphiphile Systems. *Journal of Physical Chemistry B*. 2009;113:84 - 91.
- [34] Pascual-Izarra C, Dong AW, Pas SJ, Hill AJ, Boyd B J, Drummond CJ. Advanced fitting algorithms for analysing positron annihilation lifetime spectra. *Nuclear Instruments and Methods in Physics Research A*. 2009;603:456-66.
- [35] Jain PC. Positron annihilation in liquid crystalline materials. In: Jain PC, Singru RM, Gopinathan KP, editors. *Positron annihilation: World scientific publishing Co.*; 1985. p. 692 - 5.
- [36] Singh KC. On the study of liquid crystalline materials using positron annihilation spectroscopy. *Phys Stat Sol C*. 2009;6:2482-6.
- [37] Dong AW, Fong C, Waddington LJ, Hill AJ, Boyd B J, Drummond CJ. Chain Packing and Mobility of Phospholipid Bilayers and Liposomes: Characterisation Using Positron Annihilation Lifetime Spectroscopy (PALS) Physical Chem Chem Phys. 2014;accepted.
- [38] Dong AW, Fong C, Hill AJ, Boyd B J, Drummond CJ. Probing the amphiphile micellar to hexagonal phase transition using Positron Annihilation Lifetime Spectroscopy. *Journal of Colloid and Interface Science*. 2013;402:173-9.

- [39] Jean YC, Hancock AJ. Positron lifetime studies on phase transitions of phospholipids. *The Journal of Chemical Physics*. 1982;77:5836-9.
- [40] Singer MA, Jain MK, Sable HZ, Pownall HJ, Mantulin WW, Lister MD, et al. The properties of membranes formed from cyclopentanoid analogues of phosphatidylcholine. *Biochimica et Biophysica Acta - Biomembranes*. 1983;731:373-7.
- [41] Wang YY, Hancock AJ, Jean YC. Interactions of benzoquinone with a model membrane bilayer as reported by a positronium probe. *Journal of the American Chemical Society*. 1983;105:7272-6.
- [42] Graf G, Handel ED, McMahon PL, Glass JC. Biochemical Applications of the Positron Annihilation Techniques. In: Ache HJ, editor. *Positronium and Muonium Chemistry*. Washington D.C: ACS Press; 1979. p. 67-87.
- [43] McMahon PL, Graf G, Glass JC. The phase transition in phospholipid vesicles probed by the positron annihilation lifetime technique. *Physics Letters A*. 1979;72:384-6.
- [44] McGrath AE, Morgan CG, Radda GK. Positron lifetimes in phospholipid dispersions. *Biochimica et Biophysica Acta - Biomembranes*. 1977;466:367-72.
- [45] Sane P, Salonen E, Falck E, Repakova J, Tuomisto F, Holopainen JM, et al. Probing Biomembranes with Positrons. *The Journal of Physical Chemistry B*. 2009;113:1810-2.
- [46] Ache HJ. *Chemistry of the Positron and of Positronium*. *Angewandte Chemie International Edition in English*. 1972;11:179-99.
- [47] Biatry B. Cosmetic or dermatological compsns. contg. phytantriol. L'OREAL SA. 2002:US2002048593-A1.
- [48] Compain D. Compain, D. Cosmetic/dermatological composition useful e.g. as a skin care, make-up, solar protection or hair care product, comprises an organic lipophilic UV filter and phytantriol in the form of cubic gel particles. L'OREAL SA.FR2899462-A1.
- [49] Y. S, Shah JC. *Pharm dev Technol*. 1998;3:549.
- [50] Barauskas J, Landh T. Phase Behavior of the Phytantriol/Water System. *Langmuir*. 2003;19:9562-5.
- [51] Dong YD, Dong AW, Larson I, Rappolt M, Amenitsch H, Hanley T, et al. Impurities in commercial phytantriol significantly alter its lyotropic liquid-crystalline phase behaviour *Langmuir*. 2008;24:6998-7003.
- [52] Dong AW. *Application of Positron Annihilation Lifetime Spectroscopy (PALS) to the Characterization of Nanostructure in Ordered Self-assembled Systems Melbourne Australia: PhD Thesis Monash University; 2012.*
- [53] Pascual-Izarra P, Dong AW, Pas SJ, Hill AJ, Boyd BJ, Drummond CJ. Advanced fitting algorithms for analysing positron annihilation lifetime spectra. *Nuclear Instruments and Methods in Physics Research A*. 2009;603:456-66.
- [54] Kotera K. ST, Yamanaka T. . *Physics Letters A*. 2005;345.
- [55] Duplatre G, Ferreira Marques MF, da Graca Miguel M. Size of Sodium Dodecyl Sulfate Micelles in Aqueous Solutions as Studied by Positron Annihilation Lifetime Spectroscopy. *J Phys Chem*. 1996;100:16608-12.
- [56] Geise GM, Willis CL, Doherty CM, Hill AJ, Bastow TJ, Ford J, et al. Characterization of Aluminum-Neutralized Sulfonated Styrenic Pentablock Copolymer Films. *Industrial and Engineering Chemistry Research*. 2013;52:1056-68.
- [57] Ladewig BP, Knott RB, Hill AJ, Riches JD, White JW, Martin DJ, et al. Physical and electrochemical characterisation of nanocomposite membranes of Nafion and functionalised silicon oxide. *Chem Mat*. 2007;19:2372-81.
- [58] Hill AJ. *Positron Annihilation Lifetime Spectroscopy* In: G. P. Simon E, editor. *Polymer Characterization Techniques and their Application to Blends*. NY: Oxford University Press; 2003. p. 401-35.

- [59] Choudhury SR, Yadav R, Maitra AN, Jain PC. Positron annihilation studies in CTAB reversed micellar systems. In: Dorikens-Vanpraet L, Dorikens M, Segers D, editors. Positron annihilation: World scientific publishing Co.; 1989. p. 818 - 20.
- [60] Handel ED, Ache HJ. Positronium formation in aqueous micellar solutions of sodium dodecylsulfate. *The Journal of Chemical Physics*. 1979;71:2083-7.
- [61] Jean YC, Mallon PE, Schrader DM. Principles and applications of positron & positronium chemistry. ISBN 9812381449 ed. Singapore World Scientific; 2003.
- [62] Wang YY, Jean YC. Biological applications of positron annihilation Studies in physical and theoretical chemistry. 1988;57:353-78.
- [63] Kano K, Romero A, Djermouni B, Ache HJ, Fendler JH. Characterisation of surfactant vesicles as membrane mimetic agents. 2. Temperature dependant changes of the turbidity, viscosity, fluorescence polarisation of 2-methylanthracene and positron annihilation in sonicated dioctadecyldimethylammonium chloride. *J Am Chem Soc*. 1979;101:4030-7.
- [64] Kaasgaard T., Drummond CJ. Ordered 2D and 3D nanostructured amphiphile self assembly materials stable in excess solvent. *Phys Chem Chem Phys*. 2006;8:4957-75.
- [65] Gustafsson J, Ljusberg-Wahren H, Almgren M, Larsson K. Submicron Particles of Reversed Lipid Phases in Water Stabilized by a Nonionic Amphiphilic Polymer. *Langmuir*. 1997;13:6964-71.
- [66] Larsson K. Aqueous dispersions of cubic lipid-water phases. *Current Opinion in Colloid & Interface Science*. 2000;5:64-9.
- [67] Boyd BJ, Whittaker DV, Khoo SM, Davey G. Hexosomes Formed From Glycerate Surfactants - Formulation as a Colloidal Carrier for Irinotecan. *International Journal of Pharmaceutics*. 2006;318:154-62.
- [68] Boyd BJ, Whittaker DV, Khoo S-M, Davey G. Lyotropic liquid crystalline phases formed from glycerate surfactants as sustained release drug delivery systems. *Int J Pharm*. 2006;309:218-26.
- [69] Dong AW, Fong C, Waddington LJ, Hill AJ, Boyd BJ, Drummond CJ. Chain Packing and Mobility of Phospholipid Bilayers and Liposomes: Characterisation Using Positron Annihilation Lifetime Spectroscopy (PALS)" *Phys Chem Chem Phys* 2014;accepted.
- [70] Eldrup M, Lightbody D, Sherwood JN. The temperature dependence of positron lifetimes in solid pivalic acid. *Chemical Physics*. 1981:51-8.
- [71] Mezzenga R, Meyer C, Serais C, Romonsanu AI, Sagalowicz L, Hayward RC. *Langmuir*. 2005;21:3322.
- [72] Sagalowicz L, Mezzenga R, Leser ME. *Current Opinion in Colloid & Interface Science*. 2006;11:224.
- [73] Tilley AJ, Drummond CJ, Boyd BJ. Disposition and association of the steric stabiliser pluronic F127 in lyotropic liquid crystalline nanostructured particle dispersions. *J Colloids and Interface Science*. 2013;392:288-96.
- [74] Gustafsson J, Ljusberg-Wahren H, Almgren M, Larsson K. Cubic lipid-water phase dispersed into submicron particles. *Langmuir*. 1996;12:4611-3.
- [75] Spicer PT. Progress in Liquid Crystalline Dispersions: Cubosomes. *Current Opinion in Colloid & Interface Science*. 2005;10:274-9.
- [76] Boyd BJ. Characterisation of drug release from cubosomes using the pressure ultrafiltration method. *International Journal of Pharmaceutics*. 2003;260:239-47.
- [77] Boyd BJ. Chapter 10: Controlled Release from Cubic Liquid Crystalline Particles (Cubosomes). in "Bicontinuous Structured Liquid Crystals", Spicer, P.T. and Lynch, M.L (Eds.), Taylor and Francis, Florida pp285-305 (2005).
- [78] Nguyen TH, Hanley T, Porter CJH, Larson I, Boyd BJ. Phytantriol and Glycerol Monooleate Cubic Liquid Crystalline Phases as Sustained-Release Oral Drug Delivery

Systems for Poorly Water-Soluble Drugs Ii. In-Vivo Evaluation. *Journal of Pharmacy and Pharmacology*. 2010;62:856-65.

[79] Chong JYT, Mulet X, Waddington LJ, Boyd BJ, Drummond CJ. Steric stabilisation of self-assembled cubic lyotropic liquid crystalline nanoparticles: high throughput evaluation of triblock polyethylene oxide-polypropylene oxide-polyethylene oxide copolymers. *Soft Matter*. 2011;7:4768-77.

[80] Amoozgar Z, Yeo Y. Recent advances in stealth coating of nanoparticle drug delivery systems. *Wiley Interdisciplinary reviews- nanomedicine and nanobiotechnology* 2012;4:219-33.

[81] Li JT, Caldwell KD, Rapoport N. Surface properties of Pluronic-coated polymeric colloids. *Langmuir*. 1994;10:4475-82.